Composition and size dependence of magnetic properties of FePt/Fe exchange-spring films

Yu Song, Zhe Zhang, Nian Duan, Jiawei Wang, Yuang Chen, Bei Tong, Xiaofei Yang, Yue Zhang *

School of Optical and Electronic Information, Huazhong University of Science and Technology, Wuhan 430074, Hubei, China

ARTICLE INFO

ABSTRACT

The composition and size dependence of the magnetic properties of FePt/Fe exchange-spring bilayer films was studied using micromagnetic simulation. Based on the simulated hysteresis loops for composite layers with an identical thickness of 20 nm and different composition ratios, it can be observed that when the thickness ratio of Fe is 10%, an exchange-spring effect with a negative nucleation field appears; the switching field is greatly reduced compared to the rigid magnetic FePt, and the squareness ratio reaches its maximum value. When the thickness ratio of Fe is 25% and more, the nucleation fields become positive; meanwhile, the coercivity is smaller than the switching field, and the squareness ratio decreases because of the increase in the thickness of the Fe film. In addition, at a fixed thickness ratio and total volume, the switching field of the FePt/Fe bilayer films is further reduced, accompanied by a decrease in the squareness ratio due to an increase in the thickness of the Fe layer.

© 2014 Elsevier B.V. All rights reserved.

1. Introduction

The exchange-spring effect has attracted extensive interest since the original report by Kneller [1]. Exchange-spring magnetic bilayers are composed of nanometer-scale coupled hard-magnetic (HM) and soft-magnetic (SM) films, and a reversible demagnetization behaviour in the SM phase is observed when the external field does not exceed a critical value [2–7]. Unlike conventional permanent magnetic materials, demagnetization in an exchange-spring magnet is nucleated in the SM phase, leading to a significant reduction of the switching field without affecting the thermal stability [8–11]. Therefore, the exchange-spring effect has its potential in the applications in high-performance magnetic recording [1,12–14].

Among exchange-spring magnets, the FePt/Fe bilayer has attracted great attention [15–19]. Compared to the HM FePt layer with a very high magneto-crystalline anisotropy energy, the coercivity of the FePt/Fe bilayers magnetized in the perpendicular direction is significantly smaller [20–23]. Such coercivity control has made the FePt/Fe exchange-spring magnet one of the most important potential candidates for high-density magnetic recording materials [5,24,25]. Extensive theoretical [26] and experimental [2,27–29] studies on the exchange-spring behaviour of the FePt/Fe composite layers have

been carried out. For example, it has been reported that the thickness of the SM Fe layer and the strength of the interfacial exchange coupling have a great effect on the coercivity and other magnetic properties of the FePt/Fe composite layers [26,28,29]. However, in view of future applications, more research is still necessary, as the factors that are critical to the recording performance of a storage medium not only include the thickness of the SM layer and interfacial exchange coupling, but some other aspects such as the thickness ratio, size and shape as well. All these factors need to be taken into account for optimization of the properties during the design process of the storage cell.

Therefore, at the present stage of our research, the magnetic properties of different FePt/Fe exchange-spring magnets having various shapes, sizes, and thickness ratio of FePt have been studied using the micro-magnetic simulation software known as 'object-oriented micro-magnetic framework' (OOMMF). Based on the results of the simulation, the optimum magnetic properties are understood and the related mechanisms are discussed.

2. Simulation methods

The dynamical calculations in the simulation are based on the well-known Gilbert equation,

$$\frac{\mathrm{d}\vec{M}}{\mathrm{d}t} = -\gamma \vec{M} \times \vec{H}_{\text{eff}} + \frac{\alpha}{M_{\text{S}}}\left(\vec{M} \times \frac{\partial \vec{M}}{\partial t}\right) \tag{1}$$
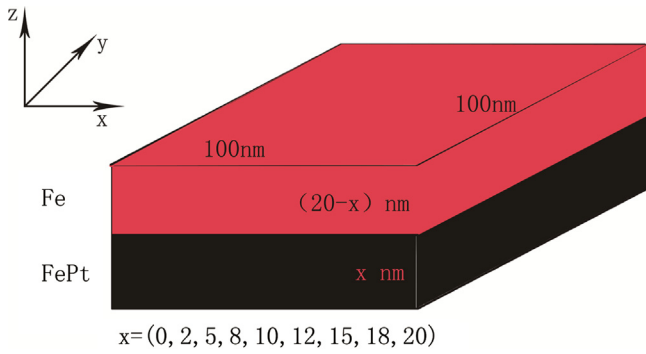
Fig. 1. The model for simulation: the FePt/Fe exchange-spring bilayer.

Table 1
Thickness of FePt/Fe layer with fixed total volume (2×10^5 nm^3) but different underside lengths.

Underside length/nm	100	80	70	60	50	40
Thickness of FePt/nm	18	28	37	50	72	113
Thickness of Fe/nm	2	3	4	6	8	12

where M is the magnetization vector; α and M_S are the damping constant and saturation magnetization, respectively; γ is the Gilbert gyromagnetic ratio; H_{eff} is the effective field including the exchange, demagnetization, anisotropy, and external magnetic fields.

As shown in Fig. 1, a cuboid composite layer composed by Fe (upper) and FePt (bottom) was chosen for the simulation. First, the magnetic properties of the FePt/Fe composite films with different thickness ratios were studied, and an optimal thickness ratio is expected to be determined. The total thickness is 20 nm while the width and the length are same of 100 nm. In this size, the thickness of each layer is around 10 nm, and the ratio of the underside length to the thickness is very large, about 10:1. Therefore, the change of the magnetization against the thickness ratio can be mainly related to the exchange spring behaviour, and the influence of the demagnetization field, can be neglected.

The size of the unit cell of the magnetic moment was 5 nm × 5 nm × 1 nm. The thickness ratio of FePt was varied from 100% to 0%. After the optimal thickness ratio of FePt was determined, the effect of the change in size on the magnetic properties was further investigated using a series of composite films with a fixed thickness ratio and volume, but with different underside lengths and thicknesses, as shown in Table 1.

The saturation magnetization (M_S) of the FePt and Fe layers is 6.9×10^5 A/m and 1.7×10^6 A/m [26], respectively, and the M_S of the composite layers can be obtained from the equation [13],

$$M_S = M_{S(\text{FePt})}f_{\text{FePt}} + M_{S(\text{Fe})}f_{\text{Fe}} \qquad (2)$$

where f_{FePt} and f_{Fe} are the thickness ratios of FePt and Fe, respectively. The magneto-crystalline anisotropy constant (K_U) of the FePt and Fe layers is 4×10^6 J/m^3 and 10^4 J/m^3 [26], respectively; the easy axis for the uniaxially anisotropic FePt and Fe is [0 0 1] and [1 0 0], respectively. The exchange constant A for Fe, FePt, and FePt/Fe interface is 10^{-11} J/m, and α is 0.01 [26]. The external magnetic field is applied along the z axis.

In the simulation process, an initial equilibrium state of the spin configuration is obtained by solving Eq. (1) without considering the external magnetic field. Then, the composite layers are simulated to be magnetized till saturation occurs, followed by the simulation of the hysteresis loops.

3. Results and discussion

3.1. The initial states of the magnetic moments in the films with different thickness ratios of FePt

The zero-field initial states of the magnetic moments are depicted in Fig. 2. It can be seen that in the HM FePt layer, most moments align along the z axis, which is the easy axis of FePt. However, in the SM Fe layer, the moments in the Fe layer that are near the FePt phase do not align along the easy axis of Fe; instead they align close to the easy axis of FePt because of the stronger anisotropy field of the FePt layer. Furthermore, θ, the angle between the magnetic moment and the z axis, increases with z. As the thickness ratio of Fe becomes 40% and more, θ can continuously change from 0° to 90°, forming an intact 90° magnetic domain wall mainly in the Fe phase.

3.2. The hysteresis loops and the magnetic properties of the composite films with different thickness ratios of FePt

The magnetic hysteresis loops for the pure FePt and composite films with 10% Fe are shown in Fig. 3(a). It can be seen that the switching field (H_S) and coercivity (H_C) for both samples coincide. For the pure FePt film, H_S is as large as 10.9915 T, which is too strong to switch the moments in the writing process. When the thickness ratio of FePt becomes 90%, H_S is significantly reduced to 2.8885 T with a clear increase in the remanent magnetization (M_r). In addition, one can see a continuous demagnetization from -0.35 T to H_S, indicating the typical exchange-spring behaviour with a negative nucleation field (H_N), -0.35 T, which signifies a critical field below which the moments will deviate from the saturation state [6]. In an exchange-spring magnet, after nucleation in the SM phase, the rotation of the SM moments approaches the HM phase in a stronger magnetic field. The moments of the
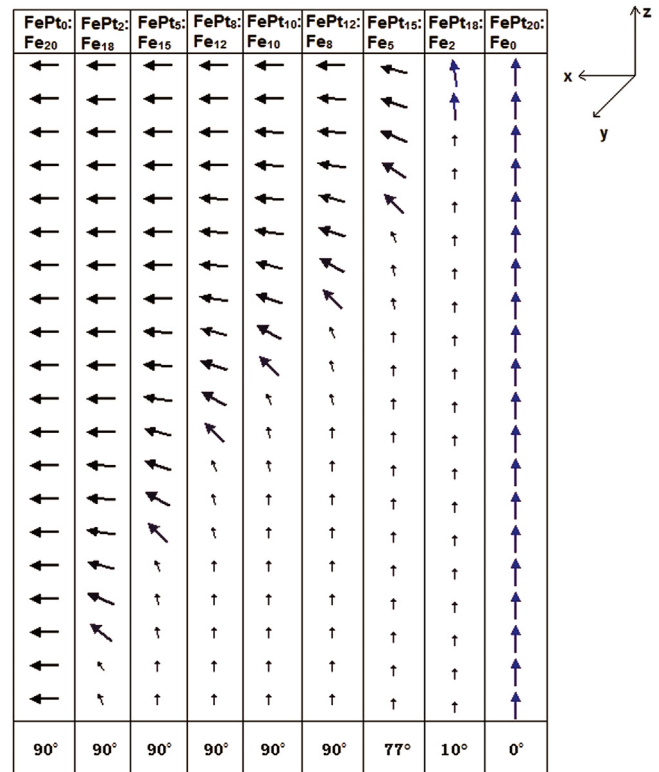

Fig. 2. The angle between the magnetic moment and the z axis with different thickness ratios of FePt in the FePt/Fe exchange-spring bilayers.
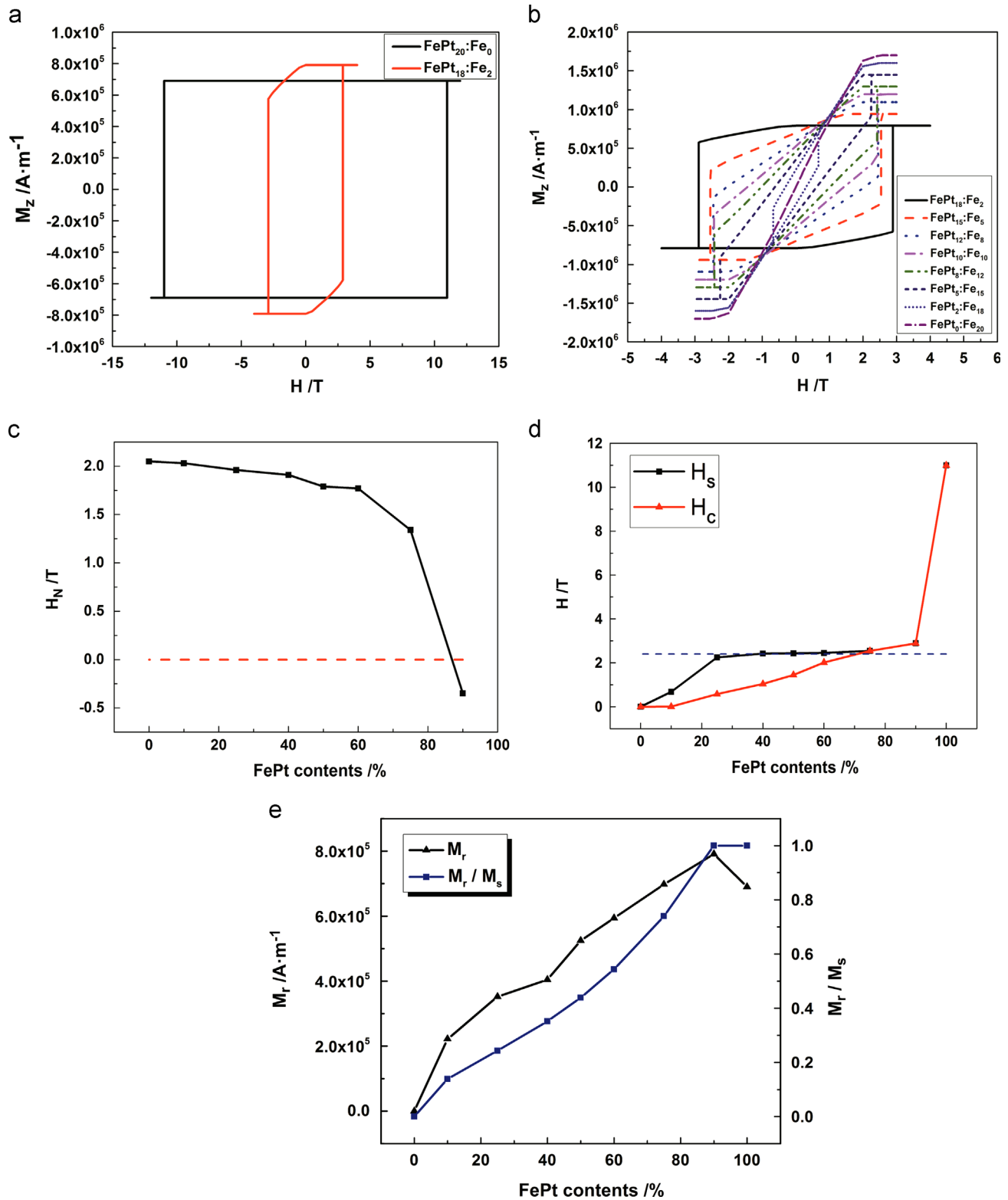
Fig. 3. (a) The magnetic hysteresis loops of the FePt/Fe bilayers with 100% and 90% of the thickness ratios of FePt; (b) the magnetic hysteresis loops for the FePt/Fe bilayers with different thickness ratios excluding the proportion 20:0; (c) the nucleation fields with different thickness ratios of FePt; (d) the coercivity and the saturation magnetization with different thickness ratios of FePt (the calculated switching field is shown by the blue dashed line); (e) the remanence and the squareness ratio with different thickness ratios of FePt. (For interpretation of the references to color in this figure legend, the reader is referred to the web version of this article.)

HM phases are reversed when the domain wall of the SM phase penetrates into the HM phase [1]. H_S reflects the critical de-pinning field for the movement of the domain wall into the HM phase [4]. Compared to single FePt films, the switching of the

FePt/Fe exchange-spring magnet is nucleated in the Fe phase, resulting in an easier reversal in the demagnetization process.

As shown in Fig. 3(b), when the thickness ratio of FePt decreases from 90% to 0%, the shapes of the hysteresis loops vary

and the SM behaviour becomes dominant. Some important magnetic parameters, such as H_N, H_C, H_S, M_r and the squareness ratio (M_r/M_S), are determined from these loops. The changes in these parameters with the thickness ratio of FePt are depicted in Fig. 3(c)–(e).

As shown in Fig. 3(c), H_N increases when the thickness ratio of FePt decreases. At this point, more magnetic moments of Fe are decoupled from FePt, and these moments can deviate from the saturated state in a higher critical field. Additionally, it is noticed that H_N becomes negative when the thickness ratio of FePt increases to 90%. In the HM/SM exchange-spring materials, a positive H_N appears only if the double layer thickness of the SM phase exceeds the exchange length (l_{ex}) of the HM phase [6], which can be determined by

$$l_{ex} = \pi \left(\frac{A_h}{K_h} \right)^{1/2} \tag{3}$$

where A_h and K_h are the exchange stiffness constant and the magneto-crystalline anisotropy constant of the hard phase, respectively. Based on Eq. (3), the l_{ex} of FePt is 4.97 nm, which is smaller than the double layer thickness of the SM Fe phase when the thickness ratio of Fe is 25% and more. From Fig. 3(d), one can see that when the thickness ratio of FePt is between 25% and 75%, a constant value of H_S is observed and H_C is smaller than H_S. As for the exchange-spring magnet composed of HM and SM phases with infinite thicknesses, H_S can be determined theoretically using the following equations [4],

$$H_S = \frac{2}{\mu_0} \frac{\left[M_1 L_2 + M_2 L_1 \left(\sqrt{1 - \frac{L_2 A_2}{L_1 A_1}} - 1 \right) \right] \sqrt{(L_1 A_1 - L_2 A_2) L_1 A_1}}{M_1^2 A_1 L_2 - (2M_1 A_1 - M_2 A_2) M_2 L_1}, (L_1 < 0) \tag{4}$$

$$L_i = K_i - \mu_0 M_i^2 / 2, (i = 1, 2) \tag{5}$$

where subscript 1 and 2 represent SM and HM, respectively; M_i is the saturation magnetization; μ_0 is the permeability of the vacuum; A_i is the exchange constant; K_i is the magneto-crystalline anisotropy constant; L_i is the effective anisotropy constant which indicates a combination of the magneto-crystalline anisotropy and the shape anisotropy. The theoretical values of H_S were calculated and are shown by the blue dashed line in Fig. 3(d). It is consistent with the constant value of H_S obtained from the simulated hysteresis loops. When the thickness ratio of either phase is very small, the theoretical H_S clearly deviates from the constant value due to the small thickness of the FePt or Fe layer.

Furthermore, when the thickness ratio of FePt is 75% and less, H_C is one-fourth or less than that of the pure FePt. In Ref. [2], a critical SM size (l_C) for such a reduction of coercivity has been presented as follows

$$l_C = \pi \left(\frac{2A}{K_h} \right)^{1/2} \tag{6}$$

Based on the related parameters, the l_C is determined to be 7.02 nm, which is close to the thickness of Fe for composite layers with the thickness ratio of FePt larger than 75%.

Fig. 3(e) depicts the variation of M_r and M_r/M_S with the thickness ratio of FePt. It can be seen that compared to pure FePt, the exchange-spring bilayers have larger M_r when the thickness ratio of FePt is between 90% and 75%, and a peak for the maximum M_r is found when the thickness ratio of FePt is 90%. Both M_r and M_r/M_S decline when the thickness ratio of FePt is less than 75%.

When the amount of Fe is very small, an intact 90° domain wall cannot be formed and the Fe moments are strongly pinned by the anisotropy field of FePt. As a result, enhanced M_r and M_r/M_S for the composite films are predicted due to the larger M_S of Fe. When the

thickness ratio of Fe is so large that its size exceeds l_C, an intact domain wall is formed, leaving some of the Fe moments outside of the domain wall. These moments are not strongly coupled to the FePt moments and can rotate easily in an external field, resulting in smaller H_C and M_r. Particularly, H_C becomes smaller than H_S when the thickness ratio of FePt is less than 75%, i.e., the rotated Fe moments can offset the FePt moments, thus creating a zero net moment in the composite layers before the reversal of the FePt moments. Taking H_S, H_C, and M_r/M_S into account, it is noticed that when the thickness ratios of FePt are 90% and 75%, M_r and M_r/M_S are large enough for information storage, but H_S is still large even
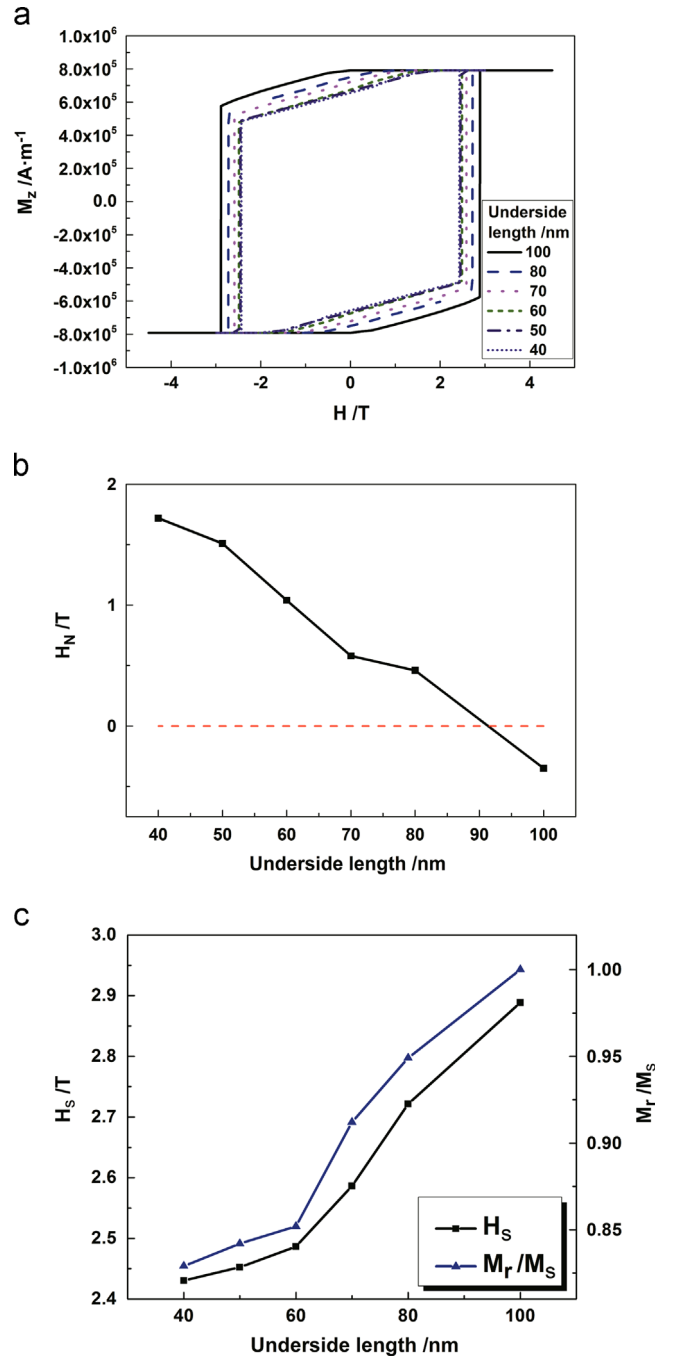

Fig. 4. (a) The magnetic hysteresis loops for different underside lengths at a fixed total volume and an optimal thickness ratio of FePt (90%); (b) the nucleation field with the variation in the underside length at an optimal thickness ratio of FePt (90%); (c) the coercivity and the squareness ratio with the variation in the underside length at an optimal thickness ratio of FePt (90%).

though it is greatly reduced as compared with the H_S of the pure FePt. On the other hand, when Fe becomes dominant in thickness ratio, H_S and H_C are further reduced, but M_r and M_r/M_S also decrease. Therefore, an effort to further improve these properties is necessary.

3.3. The hysteresis loops and the magnetic properties of the FePt90-Fe10 composite films with different sizes

At a fixed total volume (2×10^5 nm^3) and thickness ratio of FePt (90%), the impact of variations in size, including the underside length and thickness, on the magnetic properties was further investigated. The magnetic hysteresis loops are shown in Fig. 4(a); it can be seen that the areas of the loops decrease with the reduction in the underside length. H_N, H_S, and M_r/M_S determined from the loops are depicted in Fig. 4(b) and (c). From Fig. 4(b), it is observed that H_N increases with the decrease in the underside length and H_N changes from negative to positive when the underside length decreases to 80 nm. At this length, the double thickness for Fe is larger than the l_{ex} of FePt, leading to the exchange-spring effect with the positive H_N. When the thickness of the Fe layer increases further with a decrease in the underside length, more SM moments are decoupled from the moments of FePt, and these can deviate from the saturated state in a higher nucleation field. Fig. 4(c) depicts the change in H_S and M_r/M_S with the underside length, from which it can be seen that both H_S and M_r/M_S are reduced with a decrease in the underside length. When the underside length is larger than 60 nm, the change in H_S and M_r/M_S becomes smaller, corresponding to a 6-nm thickness of Fe. This result indicates that for the FePt/Fe composite film with a fixed thickness ratio of FePt, H_S can be reduced by decreasing the underside length of the composite layers, accompanied by a small decrease in M_r/M_S. As the thickness of Fe increases with the decrease in the bottom length, as discussed above, the nucleation in the SM phase and the switching in the HM phase become easier, resulting in the larger H_N and the smaller H_S and M_r/M_S. On the other hand, the changes in the shape alter the demagnetization field, which can also modify H_S and M_r/M_S due to the variation of the effective magnetic anisotropy of the HM FePt layer:

$$K_{eff} = K_a - \frac{\mu_0}{2}(N_\perp - N_{//})M_S^2 \tag{7}$$

where K_a is the magneto-crystalline anisotropy constant, and $N_\perp$ and $N_{//}$ represent the out-of-plane demagnetization factor and the in-plane one, respectively. As to the film with a small thickness and a large underside length, $N_\perp - N_{//}$ is close to 1, and it will be smaller when the thickness-to-underside length ratio becomes larger, leading to a stronger effective magnetic anisotropy energy, and a more stable out-of-plane state and a larger switching field are expected. However, the simulation result is to the contrary, indicating the dominance of the influence of thickness variations of the SM Fe layer over the demagnetization effect.

4. Conclusions

In summary, the results of the micromagnetic simulation show that with respect to 20-nm-thick pure FePt films, the switching field can be greatly reduced and the remanent magnetization increased by replacing 10% FePt with Fe due to the exchange-spring behaviour with a negative nucleation field. For the FePt/Fe composite layer with a constant total thickness (20 nm), when the thickness ratio of Fe is larger than 25%, the thickness of the Fe layer exceeds the domain-wall thickness. As a result, the exchange-spring behaviour with positive nucleation fields can be observed; the coercivity becomes smaller than the switching field

and the squareness ratio also decreases. Additionally, at a constant total volume (2×10^5 nm^3) and the optimal thickness ratio of FePt (90%), the switching field of the FePt/Fe exchange-spring bilayer films can be further reduced at the expense of the squareness ratio by reducing the bottom size.

References

[1] E.F. Kneller, R. Hawig, The exchange-spring magnet: a new material principle for permanent magnets, IEEE Trans. Magn. 27 (1991) (3588–3560).
[2] D. Suess, Micromagnetics of exchange spring media: Optimization and limits, J. Magn. Magn. Mater. 308 (2007) 183–197.
[3] T. Leineweber, H. Kronmüller, Micromagnetic examination of exchange coupled ferromagnetic nanolayers, J. Magn. Magn. Mater. 176 (1997) 145–154.
[4] G. Asti, M. Ghidini, R. Pellicelli, C. Pernechele, M. Solzi, F. Albertini, F. Casoli, S. Fabbrici, L. Pareti, Magnetic phase diagram and demagnetization processes in perpendicular exchange-spring multilayers, Phys. Rev. B: Condens. Matter 73 (2006) 094406–094421.
[5] B.Z. Chen, G.P. Zhao, H.W. Zhang, Z.Y. Zhong, 3D calculation of hysteresis loops, magnetic orientations and reversal processes for exchange-spring bilayers with perpendicular anisotropy, Physica B 407 (2012) 4574–4578.
[6] G. Asti, M. Solzi, M. Ghidini, F.M. Neri, Micromagnetic analysis of exchange-coupled hard-soft planar nanocomposites, Phys. Rev. B: Condens. Matter 69 (2004) 174401–174419.
[7] J.L. Tsai, H.W. Tai, J.C. Huang, C.S. Lin, Magnetic properties and microstructure of exchange coupled particulate films, IEEE Trans. Magn. 47 (2011) 3625–3628.
[8] G.P. Zhao, M.G. Zhao, H.S. Lim, Y.P. Feng, C.K. Ong, From nucleation to coercivity, Appl. Phys. Lett. 87 (2005) 162513.
[9] G.P. Zhao, X.L. Wang, Nucleation, pinning, and coercivity in magnetic nano-systems: an analytical micromagnetic approach, Phys. Rev. B: Condens. Matter 74 (2006) 012409–012412.
[10] D. Goll, H. Kronmüller, Critical fields of an exchange coupled two-layer composite particle, Physica B 403 (2008) 1854–1859.
[11] D. Suess, T. Schrefl, S. Fähler, M. Kirschner, G. Hrkac, F. Dorfbauer, J. Fidler, Exchange spring media for perpendicular recording, Appl. Phys. Lett. 87 (2005) 012504.
[12] X. Rui, J.E. Shield, Z. Sun, R. Skomski, Y. Xu, D.J. Sellmyer, M.J. Kramer, Y.Q. Wu, Intra-cluster exchange-coupled high-performance permanent magnets, J. Magn. Magn. Mater. 320 (2008) 2576–2583.
[13] R. Skomski, J.M.D. Coey, Giant energy product in nanostructured two-phase magnets, Phys. Rev. B: Condens. Matter 48 (1993) 15812–15816.
[14] W. Zhang, G.P. Zhao, X.H. Yuan, L.N. Ye, 3D and 1D micromagnetic calculation for hard/soft bilayers with in-plane easy axes, J. Magn. Magn. Mater. 324 (2012) 4231–4236.
[15] B. Ma, H. Wang, H. Zhao, C. Sun, R. Acharya, J. Wang, Structural and magnetic properties of a core-shell type L10 FePt/Fe exchange coupled nanocomposite with tilted easy axis, J. Appl. Phys. 109 (2011) 083907.
[16] G. Varvaro, F. Albertini, E. Agostinelli, F. Casoli, D. Fiorani, S. Laureti, P. Lupo, P. Ranzieri, B. Astinchap, A.M. Testa, Magnetization reversal mechanism in perpendicular exchange-coupled Fe/L10–FePt bilayers, New J. Phys. 14 (2012) 073008.
[17] J.L. Tsai, H.T. Tzeng, G.B. Lin, Magnetization reversal process in Fe/FePt films, Appl. Phys. Lett. 96 (2010) 032505.
[18] R. Pellicelli, C. Pernechele, M. Solzi, M. Ghidini, F. Casoli, F. Albertini, Modeling and characterization of irreversible switching and viscosity phenomena in perpendicular exchange-spring Fe–FePt bilayers, Phys. Rev. B: Condens. Matter 78 (2008) 184434–184443.
[19] D. Goll, A. Breitling, L. Gu, P.A. van Aken, W. Sigle, Experimental realization of graded L10-FePt/Fe composite media with perpendicular magnetization, J. Appl. Phys. 104 (2008) 083903.
[20] F. Casoli, F. Albertini, L. Nasi, S. Fabbrici, R. Cabassi, F. Bolzoni, C. Bocchi, Strong coercivity reduction in perpendicular FePt/Fe bilayers due to hard/soft coupling, Appl. Phys. Lett. 92 (2008) 142506.
[21] J.L. Tsai, H.T. Tzeng, B.F. Liu, Coercivity variation in exchange-coupled Fe/FePt bilayer with perpendicular magnetization, Thin Solid Films 518 (2010) 7271–7274.
[22] C.J. Aas, P.J. Hasnip, R. Cuadrado, E.M. Plotnikova, L. Szunyogh, L. Udvardi, R.W. Chantrell, Exchange coupling and magnetic anisotropy at Fe/FePt interfaces, Phys. Rev. B: Condens. Matter 88 (2013) 174409–174419.
[23] D. Goll, A. Breitling, Coercivity of ledge-type L10-FePt/Fe nanocomposites with perpendicular magnetization, Appl. Phys. Lett. 94 (2009) 052502.

[24] A. Breitling, T. Bublat, D. Goll, Exchange-coupled L10-FePt/Fe composite patterns with perpendicular magnetization, Phys. Status Solidi RRL 3 (2009) 130–132.

[25] J. Wang, B. Yang, W. Pei, G. Qin, Y. Zhang, C. Esling, X. Zhao, L. Zuo, Structural and magnetic properties of L10-FePt/Fe exchange coupled nano-composite thin films with high energy product, J. Magn. Magn. Mater. 345 (2013) 165–170.

[26] P.M.S. Monteiro, D.S. Schmool, Magnetization dynamics in exchange-coupled spring systems with perpendicular anisotropy, Phys. Rev. B: Condens. Matter 81 (2010) 214439–214445.

[27] T. Bublat, D. Goll, Large-area hard magnetic L10-FePt nanopatterns by nanoimprint lithography, J. Appl. Phys. 108 (2010) 113910.

[28] F. Casoli, F. Albertini, L. Nasi, S. Fabbrici, R. Cabassi, F. Bolzoni, C. Bocchi, P. Luches, Role of interface morphology in the exchange-spring behavior of FePt/Fe perpendicular bilayers, Acta Mater. 58 (2010) 3594–3601.

[29] L.S. Huang, J.F. Hu, J.S. Chen, Critical Fe thickness for effective coercivity reduction in FePt/Fe exchange-coupled bilayer, J. Magn. Magn. Mater. 324 (2012) 1242–1247.